

11-10-2017

Empirical Modeling of Planetary Boundary Layer Dynamics under Multiple Precipitation Scenarios using a Two-Layer Soil Moisture Approach: An Example from a Semiarid Shrubland

Zulia Mayari Sanchez-Mejia
University of Arizona

Shirley A. Papuga
Wayne State University, shirley.papuga@wayne.edu

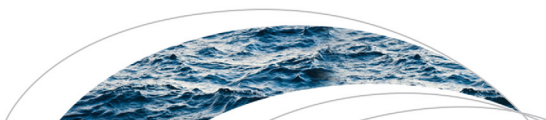
Follow this and additional works at: <https://digitalcommons.wayne.edu/geofrp>

 Part of the [Environmental Sciences Commons](#)

Recommended Citation

Sanchez-Mejia, Z. M., & Papuga, S. A. (2017). Empirical modeling of planetary boundary layer dynamics under multiple precipitation scenarios using a two-layer soil moisture approach: An example from a semiarid shrubland. *Water Resources Research*, 53, 8807–8824. <https://doi.org/10.1002/2016WR020275>

This Article is brought to you for free and open access by the Environmental Sciences and Geology at DigitalCommons@WayneState. It has been accepted for inclusion in Environmental Science and Geology Faculty Research Publications by an authorized administrator of DigitalCommons@WayneState.



RESEARCH ARTICLE

10.1002/2016WR020275

Key Points:

- Both shallow and deep soil moisture influence planetary boundary characteristics
- Planetary boundary characteristics can be estimated using empirical relationships based on soil moisture and albedo data
- Empirical relationships are coupled with two-layer soil moisture estimates to model PBL_h under current and future precipitation regimes

Correspondence to:

Z. M. Sanchez-Mejia,
zulia.sanchez@itson.edu.mx

Citation:

Sanchez-Mejia, Z. M., & Papuga, S. A. (2017). Empirical modeling of planetary boundary layer dynamics under multiple precipitation scenarios using a two-layer soil moisture approach: An example from a semiarid shrubland. *Water Resources Research*, 53, 8807–8824. <https://doi.org/10.1002/2016WR020275>


Received 15 DEC 2016

Accepted 8 SEP 2017

Accepted article online 18 SEP 2017

Published online 10 NOV 2017

Empirical Modeling of Planetary Boundary Layer Dynamics Under Multiple Precipitation Scenarios Using a Two-Layer Soil Moisture Approach: An Example From a Semiarid Shrubland

Zulia Mayari Sanchez-Mejia^{1,2}  and Shirley A. Papuga^{1,3}

¹School of Natural Resources and the Environment, University of Arizona, Tucson, AZ, USA, ²Instituto Tecnológico de Sonora, Ciudad Obregón, Mexico, ³Department of Geology, Wayne State University, Detroit, MI, USA

Abstract In semiarid regions, where water resources are limited and precipitation dynamics are changing, understanding land surface-atmosphere interactions that regulate the coupled soil moisture-precipitation system is key for resource management and planning. We present a modeling approach to study soil moisture and albedo controls on planetary boundary layer height (PBL_h). We used Santa Rita Creosote Ameriflux and Tucson Airport atmospheric sounding data to generate empirical relationships between soil moisture, albedo, and PBL_h . Empirical relationships showed that ~50% of the variation in PBL_h can be explained by soil moisture and albedo with additional knowledge gained by dividing the soil profile into two layers. Therefore, we coupled these empirical relationships with soil moisture estimated using a two-layer bucket approach to model PBL_h under six precipitation scenarios. Overall we observed that decreases in precipitation tend to limit the recovery of the PBL at the end of the wet season. However, increases in winter precipitation despite decreases in summer precipitation may provide opportunities for positive feedbacks that may further generate more winter precipitation. Our results highlight that the response of soil moisture, albedo, and the PBL_h will depend not only on changes in annual precipitation, but also on the frequency and intensity of this change. We argue that because albedo and soil moisture data are readily available at multiple temporal and spatial scales, developing empirical relationships that can be used in land surface-atmosphere applications have great potential for exploring the consequences of climate change.

Plain Language Summary Soil moisture available at different depths triggers processes that change the planetary boundary layer (PBL) height. The PBL is the closest layer of the troposphere interacting with the land surface. For instance, rainfall can change the characteristics of the soil which influences the way energy is exchanged with the atmosphere, i.e., a light-colored dry sandy soil reflects more energy (high albedo) than a darker wet sandy soil (low albedo). Using observations, we can better understand these interactions by generating models driven by empirically derived relationships. With these models, we can simulate how changes in precipitation frequency and amount could impact the dynamics of moisture in the soil and therefore the albedo of the land surface. Then, we can model how much the PBL grows and estimate the height of cloud formation. In semiarid regions, where water resources are limited and precipitation dynamics are changing, understanding these land surface-atmosphere interactions is key for resource management and planning. We argue that because albedo and soil moisture data are readily available at multiple temporal and spatial scales, developing empirical relationships that can be used in land surface-atmosphere applications have great potential for exploring the consequences of climate change.

1. Introduction

In his well-cited scenario, Charney (1975) proposed a positive feedback between the sparse desert and the dry atmosphere. Since then, for semiarid to arid regions worldwide, coupled atmosphere-vegetation models have demonstrated how small-scale land surface-atmosphere interactions can influence climate variability at the larger scales (Claussen, 1997; Henderson-Sellers, 1993; Zeng et al., 1999). Within that context, vegetation, and the lack of it, has been shown to have a strong influence on large-scale hydrological processes (e.g., Ghan et al., 1997; Hernandez et al., 2015; Sanchez-Mejia et al., 2014). Ultimately, the climate system is largely dependent on the hydrologic cycle that the vegetation influences (Chahine, 1992). In fact, studies

have suggested that small-scale positive feedbacks between vegetation and the hydrologic cycle may have the ability to elicit nonlinear responses with important large-scale consequences (Dekker et al., 2007; Rietkerk et al., 2002; Scheffer et al., 2005). Capturing the synergies between hydrologic processes at different space and time scales is necessary for modeling the influence of vegetation and the hydrologic cycle on the climate system (Chahine, 1992; Lyon et al., 2008). These synergies are often expressed through soil moisture dynamics (Chen & Dudhia, 2001). As such, soil moisture is a key link in the hydrological cycle because it couples precipitation and ecosystems (Domingo et al., 1999; Rodriguez-Iturbe, 2000; Sandeep et al., 2014; Senviratne et al., 2010).

Manabe (1969) pioneered research on better understanding the effects of soil moisture dynamics on the climate system by using a “bucket model” approach—in which a single root-zone layer is essentially a bucket of moisture. The simplicity of this bucket model, and others like it, make it an attractive method for looking at soil moisture control on ecosystem processes. For instance, ecohydrological studies have focused on using the bucket model approach for understanding ecosystem-scale evapotranspiration dynamics (e.g., Guswa et al., 2002; Porporato et al., 2004), and have linked this to transpiration and carbon assimilation (Blanken et al., 1998). Additionally, simple bucket models have been used in combination with “slab” models to look at the sensitivity of the planetary boundary layer development in relation to soil moisture heterogeneity (Chen & Dudhia, 2001; Randall et al., 2007).

The simple bucket model has been shown to adequately represent soil moisture dynamics and their influence on water cycling in ecosystems where precipitation events are large and sufficiently frequent enough to wet the entire root zone (Salvucci, 2001; Terink et al., 2015). However, in arid to semiarid ecosystems, water and carbon cycles have been shown to be controlled by soil moisture availability in two discrete layers (e.g., Breshears et al., 1997; Kurc & Small, 2007). Small precipitation events, which only wet the shallow surface layer (Sala & Lauenroth, 1982), trigger evaporation-dominated evapotranspiration (Caldwell et al., 1998; Scott et al., 2006). Large precipitation events provide soil moisture to a deeper layer (Kurc & Small, 2007; Raz-Yaseef et al., 2012) that is used toward transpiration (Cavanaugh et al., 2011) and carbon uptake (Kurc & Benton, 2010; Scott et al., 2006). Additionally, both shallow and deep soil moisture have been shown to have an effect on the surface energy budget components, albedo, and planetary boundary characteristics (Kurc & Small, 2007; Sanchez-Mejia & Papuga, 2014; Small & Kurc, 2003). Therefore, modifying the bucket model to include two-layers will be important for representing soil moisture dynamics of arid to semiarid areas in land surface-atmosphere applications.

The characteristics of the planetary boundary layer (*PBL*) reflect the effects of the surface energy dynamics of the land surface, which play a large role in the development of the climate system. For instance, higher amounts of soil moisture lead to a decreased *PBL* height, increasing the moist static energy influencing precipitation (Pal & Eltahir, 2001). Therefore, knowledge of the *PBL* height, and how it changes, is important for understanding the influence of the land surface on the climate system. Previous efforts to obtain *PBL* characteristics have tended to rely on in situ measurements (e.g., Betts & Ball, 1994; Sanchez-Mejia & Papuga, 2014) or remotely sensed products such as LiDAR or RADAR (e.g., Coen et al., 2014; Davis et al., 2000) which are not ideal for applications that need long-term and/or daily to subdaily estimates of *PBL* characteristics (Santanello et al., 2005). Alternatively, *PBL* characteristics can be explored using land surface models such as the Common Land Model (CLM) or Noah (e.g., Quintanar et al., 2008; Rihani et al., 2015; Wei et al., 2010). Notably, these models offer the ability to incorporate details, such as subsurface heterogeneities, enabling the exploration causality relationships, but these models tend to be highly complex limiting their practical utility. Furthermore, despite research efforts there is still uncertainty in numerical modeling of meteorological conditions in the *PBL* from land surface schemes (LSS) (Pleim, 2007).

Because of strong relationships between the *PBL* height and land surface characteristics such as soil moisture (Kurc & Small, 2007) and albedo (Sanchez-Mejia et al., 2014) which are generally available daily through long-term micrometeorological data sets or remote sensing products, empirical relationships that relate *PBL* height to land surface characteristics show promise (Santanello et al., 2005) for improving our understanding of *PBL* dynamics and its feedback to the climate system. A simplified empirical approach for studying *PBL* dynamics as a function of land variables could be a powerful tool for exploring land-atmosphere interactions under a variety of conditions, a task that is much more difficult and not necessarily enhanced when

using models of high complexity. This type of approach could be especially useful in understanding how *PBL* dynamics may be impacted by expected changes in precipitation regime in dryland ecosystems.

Given the sensitivity of the *PBL* to both shallow and deep soil moisture in dryland ecosystems (e.g., Sanchez-Mejia & Papuga, 2014), the objectives of this study are (1) to develop empirical methods of estimating daily *PBL* height based on readily attainable data that has been shown to influence the *PBL*, such as albedo and surface soil moisture; and (2) link the two-layer bucket model to the empirical relationships to predict changes in *PBL* dynamics under different rainfall regimes that represent potential climate change scenarios.

2. Methods

2.1. Micrometeorological, Soil Moisture, and Radiation Data

Field observations used in this study were from the Santa Rita Creosote Ameriflux site (US-SRC; <http://ameriflux.ornl.gov>) in a creosotebush-dominated shrubland (*Larrea tridentata*) located near the northern-most boundary of the Santa Rita Experimental Range (SRER) in southern Arizona. Annual precipitation at the site is bimodal and averages $\sim 350 \text{ mm yr}^{-1}$ (<http://ag.arizona.edu/SRER/data.html>), $\sim 55\%$ occurring in summer (July, August, and September) and 15% occurring in winter (December, January, and February). The mean annual surface temperature is $\sim 20^\circ\text{C}$, with monthly mean temperatures ranging from $\sim 10^\circ\text{C}$ during the winter to $\sim 35^\circ\text{C}$ during the summer. Soil is sandy loam with a 10% increase of clay and silt from 35 to 75 cm depth. Highest densities of roots are present at 10 and 35 cm in bare ground patches, while creosote bush canopy patches have their highest density at 25 cm (Sanchez-Mejia & Papuga, 2014).

Observations included 4 years of measurements (2008–2012) from an eddy covariance tower with typical micrometeorological instrumentation (Moncrieff et al., 2000; Shuttleworth, 1993). Precipitation was recorded using a tipping-bucket rain gauge. Volumetric water content was measured using *Campbell Scientific* factory-calibrated water content reflectometers at depths of 2.5, 12.5, 22.5, 37.5, and 52.5 cm replicated in six profiles, three under shrub canopies and three in bare soil patches (Sanchez-Mejia & Papuga, 2014). Incoming (SW_{in}) and outgoing (SW_{out}) shortwave radiation, as well as incoming (LW_{in}) and outgoing (LW_{out}) longwave radiation were measured with a four-component net radiometer (CNR1, Kipp & Zonen, Inc., Delft, Netherlands).

Average soil moisture at each depth was calculated based on bare ground and shrub canopy percent cover (Caldwell et al., 1998; Small & Kurc, 2003), i.e.,

$$\theta = f\theta_C + (1-f)\theta_B \tag{1}$$

where θ is volumetric soil moisture ($\text{m}^3 \text{ m}^{-3}$), f is the fraction of shrub canopy cover (14% for the US-SRC), θ_C is shrub canopy soil moisture (the average volumetric soil moisture at each depth from the three canopy profiles), and θ_B is bare soil moisture (the average volumetric soil moisture at each depth from the three bare profiles). Average soil moisture values were then aggregated for two layers: shallow (0–20 cm) and deep (20–60 cm). Aggregations were calculated as weighted averages based on the contribution of each depth:

$$\theta_{sh} = 0.33\theta_{2.5} + 0.5\theta_{12.5} + 0.17\theta_{22.5} \tag{2}$$

$$\theta_d = 0.25\theta_{22.5} + 0.375\theta_{37.5} + 0.375\theta_{52.5} \tag{3}$$

Soil moisture was then categorized into four cases based on wet and dry conditions in the upper shallow layer which is the depth subject to atmospheric demand (Boulet et al., 1997; van Keulen & Hillel, 1974; Yamanaka & Yonetani, 1999) and the (site specific) lower deep layer that comprises the majority of root zone: Case 1 corresponds to a dry shallow and dry deep layer, Case 2 corresponds to a wet shallow and dry deep layer, Case 3 corresponds to a wet shallow and wet deep layer, and Case 4 corresponds to a dry shallow and wet deep layer. The wet and dry condition in each layer was determined based on thresholds derived based on soil moisture observations at the site (Sanchez-Mejia & Papuga, 2014). Soil moisture thresholds for our site were identified for the ecosystem based on percent shrub cover using 2009–2011 data (equation (1)); shallow = 0.1229 deep = 0.1013). For each day, these thresholds are then used to categorize soil moisture into one of the four Cases.

Half-hourly surface albedo (α) was calculated as the ratio of outgoing to incoming shortwave radiation, i.e.,

$$\alpha = \frac{SW_{out}}{SW_{in}} \quad (4)$$

For albedo, midday averages, as opposed to daily averages, were calculated from 30 min data. We used midday averages (10:00 A.M. to 2:00 P.M., UTC/GMT-7, Mountain Standard Time, no daylight savings) because we assume that this is the time when available energy is at its maximum and incoming shortwave radiation is relatively stable (Arya, 2001).

We note that the source area for these measurements is inherently smaller than for the atmospheric sounding data and therefore interpretation of the results must be exercised with the understanding of that caveat.

2.2. Atmospheric Sounding Data

Atmospheric sounding data were obtained from the Department of Atmospheric Science, University of Wyoming (<http://weather.uwyo.edu/upperair/sounding.html>). The sounding data correspond to the National Weather Service surface Tucson station (KTUS, WMO: 72274) located at the Tucson International Airport (UTM: 12 R 504112, 3555012). In this study, we analyzed the *PBL* characteristics using sounding data at 00 UTC (Coordinated Universal Time; 5 P.M. local time). Variability of *PBL* height during the day is complex, from nighttime (stable conditions) to afternoon (convective conditions) and during seasons. When using potential temperature (θ_p) as a method to estimate *PBL* height, the maximum *PBL* is estimated in the afternoon (end of midday to sunset) (Seidel et al., 2010). We make the reasonable assumption that estimations using 00UTC give a good estimate of *PBL* height at its maximum during the day.

Planetary boundary layer height (PBL_h) was determined by analyzing potential temperature (θ_p) profiles (Stull, 1988) as described below. In a mixed layer, θ_p remains constant with height, and therefore the height of the *PBL* can be determined by $\Delta\theta_p/\Delta z$, where θ_p is calculated as follows:

$$\theta_p = T \left(\frac{p_0}{p} \right)^{R/c_p} \quad (5)$$

where θ_p (K) is the potential temperature, T (K) is temperature at each level, p_0 (Pa) is pressure at sea level, p (Pa) is pressure at each level, R is assumed to be $\cong Rd = (287 \text{ J K}^{-1} \text{ kg}^{-1})$ and $c_{pd} \cong 1,004 \text{ (J K}^{-1} \text{ kg}^{-1})$. The PBL_h is assumed to be the point at which $\Delta\theta_p/\Delta z \neq 0$; an example is presented in Sanchez-Mejia and Papuga (2014).

Atmospheric stability (γ_{ML} ; K m^{-1}) in the mixed layer relates to the change of θ_p with height; the thermal *PBL* development is influenced by this parameter (Santanello et al., 2005). We calculated stability as:

$$\gamma_{ML} = \frac{\theta_{pt} - \theta_{ps}}{h_t - h_s} \quad (6)$$

where θ_p is potential temperature (K), h is height (m), t refers to the top of *PBL*, and s to the surface just above the inversion zone (Santanello et al., 2005).

2.3. Development of Empirical Relationships

Data for the development of empirical relationships were selected based on soil moisture dynamics defined by the Cases (described in section 2.1). From 2008 to 2011, we identified the days corresponding to each Case and selected representative days for each Case when surface and sounding data were both available. This resulted in a total of 101 days for use in developing the empirical relationships, (i.e., $N_{\text{Case}1} = 30$, $N_{\text{Case}2} = 7$, $N_{\text{Case}3} = 32$, $N_{\text{Case}4} = 32$). Case 2 occurred infrequently, and therefore comparisons must be made cautiously in this analysis. For these 101 days, we obtained atmospheric soundings (section 2.2), shallow and deep soil moisture (section 2.1), and albedo (section 2.1). We used these data to develop empirical relationships between the land surface and the PBL_h using a polynomial approach.

Santanello et al. (2005) developed an empirical relationship between the PBL_h and soil moisture and stability for their site in the southern Great Plains using a second-order polynomial:

$$PBL_h(\theta, \gamma_{ML}) = p_0 + p_1 \gamma_{ML} + p_2 \theta + p_3 \gamma_{ML}^2 + p_4 \theta \gamma_{ML} + p_5 \theta^2 \quad (7)$$

where $p_0 \dots p_5$ are the polynomial coefficients. Using atmospheric stability (equation (6)) and shallow soil moisture (equation (2)), we adapted this empirical relationship for our site using all of days of data from 2008 to

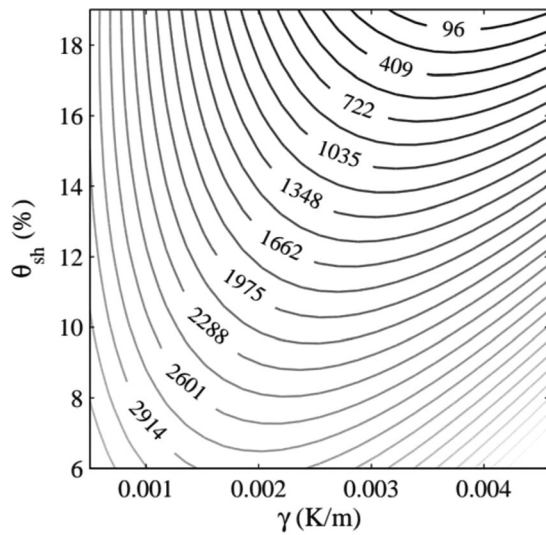


Figure 1. Planetary boundary layer height PBL_h (m) estimated as a function of shallow soil moisture (θ_{sh}) and atmospheric stability.

2011 (Figure 1) and also by categorizing the data by Case as described above (Figure 2). We report our site-specific coefficients in Table 1.

Because previous studies have highlighted the sensitivity of PBL_h to albedo and soil moisture, including deep soil moisture (Basara & Crawford, 2002), and because albedo is a more readily available parameter than PBL_h stability (Sanchez-Mejia & Papuga, 2014), we also develop an empirical relationship between the PBL_h and shallow soil moisture (equation (2)) and albedo (equation (4)) using the second-order polynomial approach (Figure 3), i.e.,

$$PBL_h(\theta_{sh}, \alpha) = p_0 + p_1\theta_{sh} + p_2\alpha + p_3\theta_{sh}^2 + p_4\theta_{sh}\alpha + p_5\alpha^2 \quad (8)$$

We also develop an empirical relationship between the PBL_h and shallow soil moisture (equation (2)) and deep soil moisture (equation (3)) using the second-order polynomial approach (Figure 3), i.e.,

$$PBL_h(\theta_{sh}, \theta_d) = p_0 + p_1\theta_{sh} + p_2\theta_d + p_3\theta_{sh}^2 + p_4\theta_{sh}\theta_d + p_5\theta_d^2 \quad (9)$$

These relationships are developed using all of 101 days of Case data from 2008 to 2011; we report the polynomial coefficients in Table 1.

Last, we develop a second-order polynomial empirical relationship using both shallow (equation (2)) and deep soil moisture (equation (3)) with albedo (equation (4)):

$$PBL_h(\theta_{sh}, \theta_d, \alpha) = p_0 + p_1\theta_{sh} + p_2\theta_d + p_3\alpha + p_4\theta_{sh}\theta_d + p_5\theta_{sh}\alpha + p_6\theta_d\alpha + p_7\theta_{sh}^2 + p_8\theta_d^2 + p_9\alpha^2 \quad (10)$$

and report the polynomial coefficients in Table 1.

2.4. Two-Layer Bucket Model of Soil Moisture Dynamics

To model shallow and deep soil moisture dynamics, we modified the standard root zone bucket model (Blanken et al., 1998; Guswa et al., 2002; LeMone et al., 2007; Rodriguez-Iturbe et al., 1999a) into a two-layer

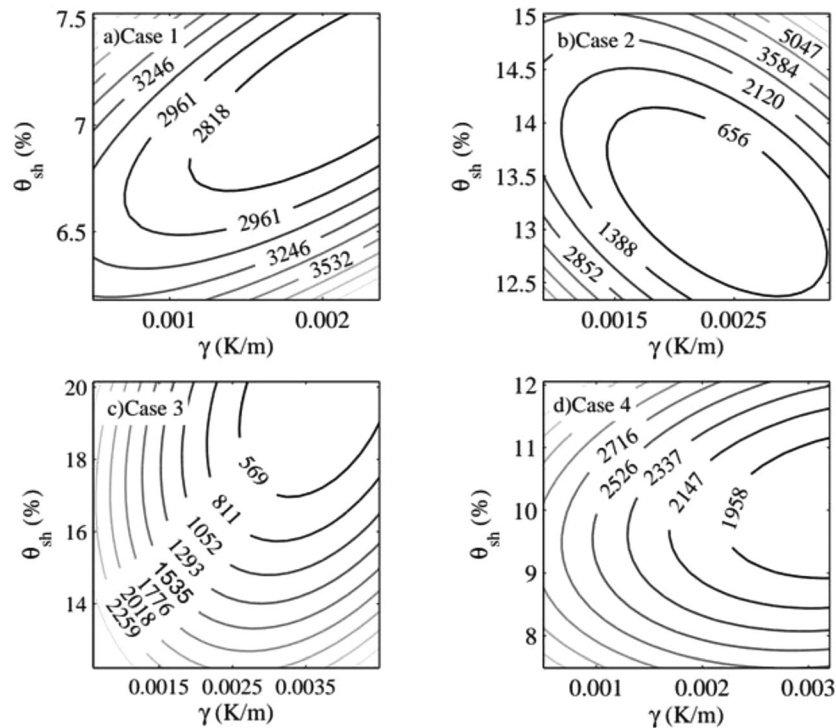


Figure 2. Planetary boundary layer height PBL_h (m) estimated as a function of shallow soil moisture (θ_{sh}) and atmospheric stability (γ_{ML}) for (a) Case 1, (b) Case 2, (c) Case 3, and (d) Case 4.

Table 1
Coefficients of Second-Order Polynomial Empirically Derived Relationships

	R ²	p ₀	p ₁	p ₂	p ₃	p ₄	p ₅
PBL _h (γ _{ML} , θ _{sh})	0.54	4.23 × 10 ³	-5.24 × 10 ⁵	-9.30 × 10 ¹	2.55 × 10 ⁸	-7.72 × 10 ⁴	3.81 × 10 ⁰
Case1 PBL _h (γ _{ML} , θ _{sh})	0.36	5.74 × 10 ⁴	5.59 × 10 ⁶	-1.69 × 10 ⁴	3.13 × 10 ⁸	-9.65 × 10 ⁵	1.32 × 10 ³
Case2 PBL _h (γ _{ML} , θ _{sh})	0.97	2.87 × 10 ⁵	-2.48 × 10 ⁷	-3.89 × 10 ⁴	1.24 × 10 ⁹	1.43 × 10 ⁶	1.34 × 10 ³
Case3 PBL _h (γ _{ML} , θ _{sh})	0.51	1.16 × 10 ⁴	-5.04 × 10 ⁵	-1.04 × 10 ³	2.42 × 10 ⁸	-6.38 × 10 ⁴	3.21 × 10 ¹
Case4 PBL _h (γ _{ML} , θ _{sh})	0.38	1.62 × 10 ⁴	-2.39 × 10 ⁵	-2.78 × 10 ³	1.31 × 10 ⁸	-6.58 × 10 ⁴	1.49 × 10 ²
PBL _h (θ _{sh} , α)	0.39	-3.01 × 10 ⁴	7.54 × 10 ²	3.17 × 10 ⁵	-3.26 × 10 ⁰	-4.42 × 10 ³	-7.32 × 10 ⁵
PBL _h (θ _{sh} , θ _d)	0.40	2.24 × 10 ³	2.39 × 10 ¹	-1.11 × 10 ²	1.38 × 10 ¹	-5.20 × 10 ¹	4.71 × 10 ¹
PBL _h (θ _{sh} , θ _d , α)	0.43	p ₀ = -3.73 × 10 ⁴ , p ₁ = 1.03 × 10 ³ , p ₂ = 6.04 × 10 ² , p ₃ = 3.34 × 10 ³ , p ₄ = -1.04 × 10 ² , p ₅ = -3.06 × 10 ¹ , p ₆ = -4.98 × 10 ¹ , p ₇ = 1.92 × 10 ¹ , p ₈ = 8.08 × 10 ¹ , p ₉ = -6.76 × 10 ¹					

bucket model (Figure 4). In this two-layer bucket model, the root zone is divided into a shallow layer where evaporation drives soil moisture and a deep layer where transpiration controls soil moisture. Leakage is allowed to occur from the shallow to the deep layer, but no redistribution is allowed from the deep to the shallow layer. The following equations describe this two-layer bucket model:

$$nZ_E \frac{ds_E}{dt} = I_{(s_E,t)} - E_{(s_E)} - L_{(s_E)} \tag{11}$$

$$nZ_T \frac{ds_T}{dt} = L_{(s_E)} - T_{(s_T)} - L_{(s_T)} \tag{12}$$

where, n is porosity, Z_E is the depth of the shallow layer, Z_T is the depth of the deep layer, s_E is the relative soil moisture content in the shallow layer, s_T is the relative soil moisture content in the deep layer, $I_{(s_E,t)}$ is the rate of infiltration, $E_{(s_E)}$ is the rate of evaporation, $T_{(s_T)}$ is the rate of transpiration, $L_{(s_E)}$ is the rate of leakage from the shallow to the deep layer, and $L_{(s_T)}$ is the rate of leakage from the deep layer out of the system. Parameters used for our specific study site are listed in Table 2.

Similar to estimating evapotranspiration in the standard bucket model, losses from the system due to evaporation $E_{(s_E)}$ and transpiration $T_{(s_T)}$ are described as piecewise functions of s_E and s_T , where s_E and s_T are constant above a certain s^* and decrease linearly to the hygroscopic point s_h in the case of E (Guswa et al., 2002) and to the wilting point s_w in the case of T (Guswa et al., 2002; Laio et al., 2001), i.e.,

$$E_{(s_E)} = \begin{cases} 0 & s_E \leq s_h \\ E_{\max} \frac{s_E - s_h}{s^* - s_h} & s_h < s_E < s^* \\ E_{\max} & s^* < s_E \leq 1 \end{cases} \tag{13}$$

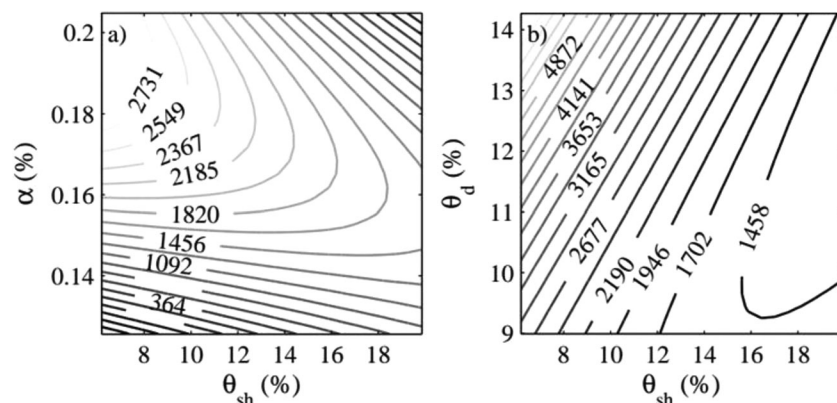


Figure 3. Planetary boundary layer height PBL_h (m) estimated as a function of (a) shallow soil moisture (θ_{sh}) and albedo (α) and (b) deep soil moisture (θ_d) and albedo.

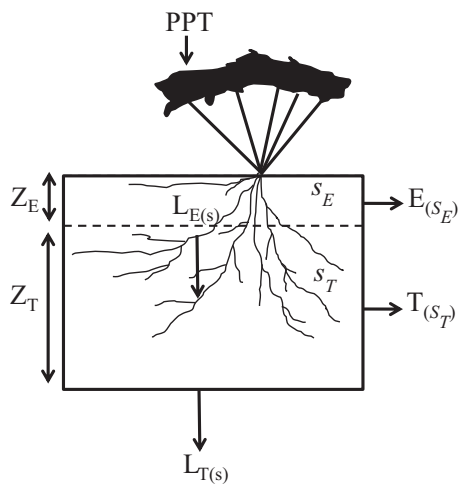


Figure 4. Modified two-layer bucket model.

$$T_{(s_T)} = \begin{cases} 0 & s_T \leq s_w \\ T_{max} \frac{s_T - s_w}{s^* - s_w} & s_w < s_T < s^* \\ T_{max} & s^* < s_T \leq 1 \end{cases} \quad (14)$$

where E_{max} and T_{max} are the maximum daily rates under wet conditions (Guswa et al., 2002). Parameters used for our specific study site are listed in Table 2.

Previous studies in similar ecosystems have shown that leakage below the root zone (60–80 cm) is rare (Liu et al., 1995), or suggest that the lower layer never gets wet enough to leak. However, in our analysis, we also include a downward only leakage term from the deep layer in our model to represent movement. Two components comprise leakage in our model: (1) hydraulic conductivity and (2) a simple empirically derived linear relationship regulating water movement out of the layer, i.e., 1% of the soil moisture in the shallow layer is moved into the deep layer and the soil moisture in the deep layer is moved out of the bottom driven by the hydraulic conductivity. We ignore hydraulic redistribution (e.g., Ryel et al., 2004; Scott et al., 2008) between the layers in part due to lack of information of this mechanism for our study site. As such, leakage is modeled as a simple linear relationship (Blanken et al., 1998):

$$L_{(s_E)} = K_{sat} s_E^{2b+3} + (0.01 \times s_E \times Z_E) \quad (15)$$

$$L_{(s_T)} = K_{sat} s_T^{2b+3} \quad (16)$$

where, K_{sat} is saturated hydraulic conductivity in cm d^{-1} and b is the exponent of the retention curve $\Psi_s = \bar{\Psi}_s s^{-b}$ where $\bar{\Psi}_s$ is the soil water potential at saturation (Caylor et al., 2005; Clapp & Hornberger, 1978). Parameters used for our specific study site are listed in Table 2.

2.4.1. Model Parameters

The depth of the shallow layer Z_E is set as 0–20 cm to minimize the influence of atmospheric demand on the deep layer (Table 2). A root density profile has been developed for this shrubland site and is reported in (Sanchez-Mejia & Papuga, 2014). As has been seen in a similar shrubland (Kurc & Small, 2007), while roots

Table 2

Parameters Used in Two-Layer Bucket Model Based on Vegetation and Soil Similar to Our Study Site

Symbol	Value	Selection source
<i>Layer depth</i>		
Z_E	0–20 cm	Estimated from root profiles
Z_T	20–60 cm	Estimated from root profiles
<i>Soil parameters</i>		
n	0.435	Cosby et al. (1984)
K_{sat}	80 cm d^{-1}	Laio et al. (2001)
b	4.9	Caylor et al. (2005)
s^* (estimated)	0.34	Caylor et al. (2005) and Clapp and Hornberger (1978)
s_{fc}	0.56	Laio et al. (2001)
s_h	0.14	Laio et al. (2001)
s_w (estimated)	0.20	Caylor et al. (2005) and Clapp and Hornberger (1978)
<i>Atmospheric loss parameters</i>		
E_{max}	0.45 cm d^{-1}	Moran et al. (2009) and Reynolds et al. (2000)
T_{max}	0.5 cm d^{-1}	Villegas et al. (2010)

Note. The selection source describes where parameter was derived.

Table 3
Number of Days for Each Case Applying Two-Layer Soil Moisture Conceptual Framework to Classify Observed and Model Data

	Case 1	Case 2	Case 3	Case 4
Ecosystem				
Observed	587	64	241	120
Model	934	125	31	5

Note. Ecosystem refers to ecosystem-averaged soil moisture.

were found to depths of 1 m in both the bare and canopy areas of our shrubland, the highest root densities were found above 60 cm. Therefore, a maximum depth of 60 cm, i.e., where the depth of the deep layer is set as $Z_T = 20\text{--}60$ cm, was used in our modeled scenarios.

Soil texture at our study site classified as a sandy loam (Kurt & Benton, 2010), and therefore we assigned a porosity (n) of 0.435 (Table 2). The parameters s_{fc} , s_{hr} , s_{wr} , and s^* can be estimated based solely on soil texture (Clapp & Hornberger, 1978; Laio et al., 2001) However, these parameters depend on both vegetation and soil properties (Guswa et al., 2002), and the two-layer bucket model can be very sensitive to

these parameters. Therefore, while we adopt soil texture-based s_{fc} and s_h (Table 3; Laio et al., 2001), we estimated s_w and s^* based on local vegetation following (Caylor et al., 2005; Clapp & Hornberger, 1978).

Partitioning evapotranspiration into its components of transpiration and evaporation is a challenging enterprise, and has not been fully conducted at our shrubland site. Because we do not have site-specific partitioning measurements, we defined the model parameters of maximum evaporation from the shallow layer and maximum transpiration from the deep layer based on research conducted in similar semiarid ecosystems (Caldwell et al., 1998; Moran et al., 2009; Reynolds et al., 2000; Villegas et al., 2010). Using these studies, we define an individual maximum value for evaporation and transpiration (Table 2).

2.4.2. Model Performance

The water from precipitation enters the shallow layer of the model as:

$$s_{Ei} = s_{Ei-1} + \frac{PPT_i}{nZ_E} \tag{17}$$

where i corresponds to the time step and PPT is precipitation.

We calibrated the two-layer model using three years (2009–2011) of daily precipitation from the micrometeorological tower as input and compared observed soil moisture in the shallow and deep layers to modeled soil moisture (Figure 5). We note that the model initialization results in a lag at the beginning of the modeling time series which is resolved as moisture accumulates. Linear regression between observations and model output suggest that shallow moisture dynamics ($R^2 = 0.62$) are better captured than deep moisture dynamics ($R^2 = 0.28$). In general however, both the modeled shallow and deep soil moisture follow the trends in peaks and dry down periods of the observed data. We note that this has consequences for the development of Cases and the use of our Case thresholds (Table 3); for instance, observed Case 1 days total 587, while modeled Case 1 days total 934 and observed Case 3 days total 241 while modeled Case 3 days total 31.

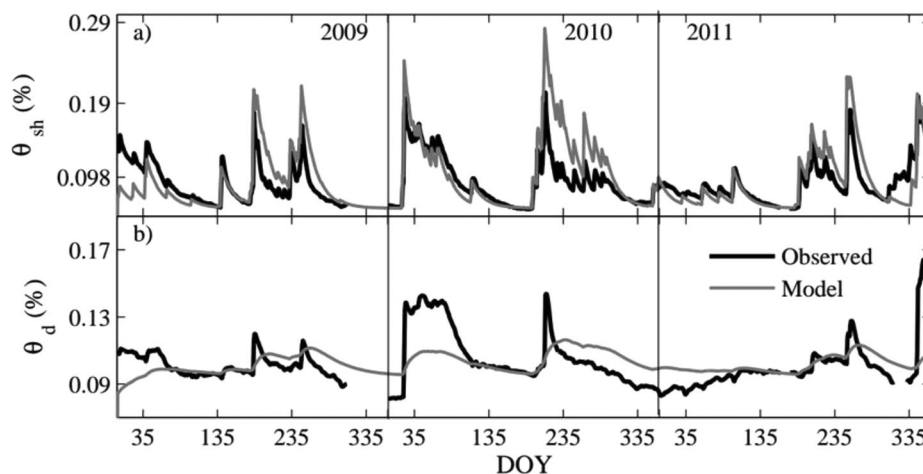


Figure 5. Two-layer bucket (a) SRER observed precipitation, (b) shallow soil moisture model versus observed $R^2 = 0.62$, (c) deep soil moisture model versus observed $R^2 = 0.28$.

Table 4
Frequency (λ) and Total Precipitation for Each Season (δ) Determined From 33 Years of Precipitation From DAYMET

	Frequency (days)	Depth (mm)
Winter	6.09	88.03
Spring	16.07	45
Summer	3.14	194.45
Fall	10.09	48.36

2.4.3. Precipitation Scenarios

While changes in precipitation regime are expected (Kunkel et al., 2013; Miller et al., 2009; Weltzin et al., 2003), the type of change is much less agreed upon. Therefore, uncertainty also remains on how these changes could influence local-scale processes (Garfin et al., 2014), such as land surface—atmosphere interactions and feedbacks. Here we analyzed six potential scenarios for precipitation (hereafter S1–S6):

1. S1: Current precipitation regime;
2. S2: A 20% decrease in overall precipitation (Garfin et al., 2014; NAST & USGCRP, 2000);
3. S3: A 20% decrease in overall precipitation and a 30% decrease in frequency (Kunkel et al., 2013);
4. S4: A 20% decrease in overall precipitation and a 30% increase in frequency;
5. S5: A 12% decrease in winter precipitation (Trenberth et al., 2003); and
6. S6: A 20% increase in winter precipitation and a 20% decrease in summer precipitation (Griffin et al., 2013; Gutzler, 2000).

To develop soil moisture Cases to link to *PBL* dynamics under these different scenarios, we modeled precipitation input as a stochastic process (Blanken et al., 1998; Rodriguez-Iturbe et al., 1999b), taking into account seasonality. At a scale where soil-moisture recycling can be neglected, the rainfall input can be generated as an external force independent from the soil moisture state (Laio et al., 2001). The response of vegetation and therefore land surface-*PBL* interactions in a water-limited ecosystem is tightly coupled to the stochastic nature of soil moisture given by precipitation (Katul et al., 2007). Because of this, rainfall follows a series of “events” in time with frequency (λ) and depth (δ) following a typical Poisson process (Bonser et al., 1985), and therefore the frequency in time is found using a typical Poisson distribution:

$$P_x(x) = \frac{(\lambda t)^x \exp^{-\lambda t}}{x!} \tag{18}$$

where, $P_x(x)$ is the probability of observing x events in a time period and λ is equal to the average rate of occurrence of the event and its dynamic with seasonality.

The depth (δ) of the precipitation event can be calculated by using an exponential function based on the average rainfall amount (Laio et al., 2001; Porporato et al., 2002). Frequency at the site was calculated from thirty three years of daily DAYMET data (1980–2013; Thornton et al., 2014), tile no. 10835. Because of the seasonality in the precipitation regime we estimated λ and δ for winter (December, January, and February), spring (March, April, May, and June), summer (July, August, and September), and fall (October and November) (Table 4).

Using these precipitation regimes as inputs into the two-layer bucket model, we obtain a daily soil moisture value for both the shallow (equation (11)) and the deep layer (equation (12)) and using percent cover, we calculate ecosystem soil moisture as a weighted average (equation (1)). Because one of our objectives was to explore how soil moisture scenarios resulting from different precipitation regimes influences atmospheric processes via albedo and PBL_h , we estimate albedo using a linear relationship from Sanchez-Mejia and Papuga (2014) and then used our empirical relationship (equations (8)–(10)) to estimate the PBL_h . We note that here while that the albedo input into the empirical model is not independent from soil moisture, the empirical models were developed using independent measures of albedo and soil moisture.

3. Results and Discussion

3.1. Soil Moisture and Albedo Influence on the Planetary Boundary Layer Height

Our analysis takes advantage of a two-layer soil moisture conceptual framework. Using this framework, we categorize our time series data into four soil moisture Cases based on wet and dry conditions in a shallow and deep soil layer. By binning days into each of these categories (Figure 6a), we can see that the PBL_h is sensitive to the soil moisture-derived cases. Overall, the PBL_h is largest when the shallow layer is dry (Cases 1 and 4) and smallest when the shallow layer is wet (Cases 2 and 3). A recent study (Sanchez-Mejia & Papuga, 2014) has shown that wet conditions in the deep layer does tend to shrink the PBL_h ; for Case 3 the PBL_h is generally lower than for Case 2 and for Case 4 the PBL_h is generally lower than for Case 1 (Figure 6a). Shallow soil moisture is highest for Case 2 and Case 3—but it is particularly higher in Case 3 (Figure 6b),

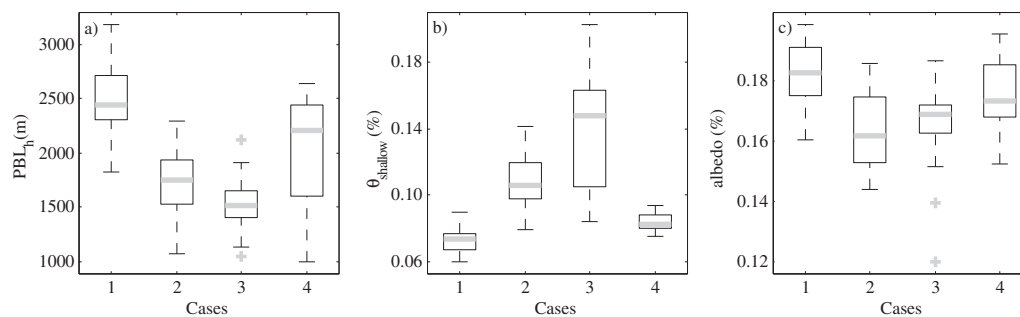


Figure 6. The variability in (a) planetary boundary layer height (PBL_h), (b) shallow soil moisture, (c) deep soil moisture, and (d) albedo with respect to Cases 1–4.

which likely is influencing the decrease of the PBL_h under that moisture condition. Albedo is lowest in Case 2 and Case 3 (Figure 6c), which supports the notion that surface soil moisture influences albedo (Sanchez-Mejia & Papuga, 2014; Small & Kurc, 2003) which is influencing the PBL_h (Jackson et al., 1976). We note that the scale at which soil moisture and albedo is measured in comparison to an atmospheric sounding is a source of uncertainty in our analysis. For instance, spatial variability in soil moisture associated with terrain can introduce complexity during moist periods at multiple scales (Western et al., 1999), having an influence on surface fluxes and ultimately the PBL (Giorgi & Avissar, 1997).

3.2. Empirical Relationships for Estimating Planetary Boundary Layer Height

Based on a statistical analysis, Santanello et al. (2007) found the need to develop empirical relationships that focused on observable properties of the PBL and the land surface rather than a model of complex processes. Further, they emphasize using daily variability in these properties, using the PBL as an integrator of surface conditions at the regional scale. A statistical analysis found that the PBL was most sensitive to atmospheric stability γ_{ML} , and that soil moisture θ also played a significant role. Therefore, they developed an empirical relationship to estimate PBL_h from daily γ_{ML} and θ (equation (7)). Because the empirical relationship only captured about 60% of the variance between the variables, the predicted range of PBL_h was smaller than the actual range, which did have consequences when using those PBL_h estimates in other applications. We do note that the atmospheric sounding from which PBL_h is estimated has a larger source area than θ , therefore a difference between the actual and predicted PBL_h is not necessarily unexpected.

Based on their findings, we calculated the γ_{ML} for our site (equation (6)) and obtained our coefficients (Table 1) for their empirical relationship for PBL_h using γ_{ML} and $\theta_{shallow}$ (equation (7); Figure 1). Using this approach, the variables explained about 50% of the variance in PBL_h ; the estimated PBL_h values fall between 298 m to about 4,600 m (Figure 1), whereas the actual PBL_h values have a range from about 300 m to about 4,600 m with a majority of those between 1,500 and 2,500 m (Figure 6a). When we look at these by Case (Figure 2), we see that the estimations for PBL_h improve for the Cases when shallow soil moisture is present, i.e., Case 3 ($R^2 = 0.51$) and Case 2 ($R^2 = 0.97$). Additionally, the differences in ranges between the actual PBL_h values (Figure 6a) and the estimated PBL_h values (Figure 1) almost disappear for these Cases.

Despite reasonable predictions of PBL_h using γ_{ML} and θ , we calculated γ_{ML} using atmospheric sounding data and therefore we presume that this parameter is not any easier to access than the PBL_h itself (Table 1 and Figures 1–3). Strong relationships between PBL_h and albedo and PBL_h and soil moisture in both the shallow and deep layer have been previously identified (Basara & Crawford, 2002). There is value in having identified these relationships in part because observations of albedo and soil moisture are readily available at multiple temporal and spatial scales (Asbjornsen et al., 2011; Wang et al., 2012)—ranging from micrometeorological data sets (Baldocchi et al., 2001; Mueller et al., 2011) to remotely sensed data (Mills, 1990; Nemani et al., 1993). Furthermore, soil moisture has been predicted from albedo (Jackson et al., 1976; Zhao & Li, 2015) and vice versa.

To explore the ability to predict PBL_h using these readily available parameters, we adopted the polynomial approach of Santanello et al. (2005). We developed an empirical relationship to estimate PBL_h from daily observations of α and $\theta_{shallow}$ (equation (8)), from daily observations of θ_{sh} and θ_d (equation (9)), and from daily observations of α , θ_{sh} and θ_d (equation (10)) (US-SRC; <http://ameriflux.ornl.gov>). Our analysis shows that α and θ_{sh} explained about 40% of the variance in PBL_h (Figure 7a). From the surface contours (Figures 1–3), we see that PBL_h increases with more shallow soil moisture and less stability (Figure 1), when soil

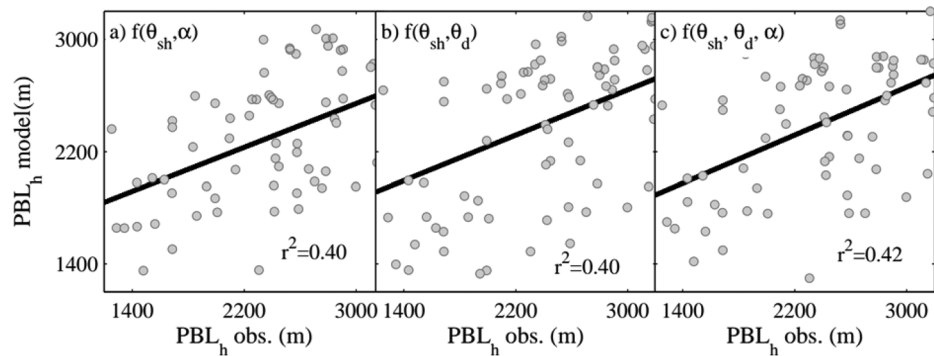


Figure 7. Observed versus model PBL_h as a function of (a) shallow soil moisture and albedo, (b) shallow and deep soil moisture, and (c) shallow and deep soil moisture and albedo.

moisture decreases and albedo increases it also develops more (Figure 2), and despite the fact that deep soil moisture is present if there is a lack of shallow moisture it develops more (Figure 3). This is expected because under these conditions, energy is partitioned toward more sensible heat flux (Otterman et al., 1993). Estimating PBL_h with θ_{sh} and θ_d did not show improvement ($R^2 = 0.40$; Figure 7b); however, a slight improvement was found using α , θ_{sh} , and θ_d ($R^2 = 0.42$; Figure 7c). The addition of deep moisture does not necessarily improve the predictability of the PBL_h , in our analysis. We suspect this is in part due to the lack of the ability of the model to adequately capture deep moisture dynamics. That being said, deep moisture data are not as readily available as shallow soil moisture, e.g., remotely sensed soil moisture generally only captures the near-surface signal (e.g., Calvet & Noilhan, 2000). Therefore, based on the availability of the variables and their influence on the PBL_h , we suggest that the empirical relationship predicting PBL_h from α and θ_{sh} (equation (8)) is a reasonable approach.

It should be noted again that the consideration of scale will be important in the derivation and use of these empirical relationships. This is because atmospheric soundings represent a scale on the order of 10 km^2 , while flux towers generally represent a scale on the order of 100 m^2 (Asbjornsen et al., 2011; Shuttleworth, 2012). How much these empirical models represent the land surface that is linked to the PBL will depend on surface heterogeneity and the response of the PBL to integrated fluxes over a larger spatial scale.

3.3. Influence of Change in Precipitation Regime on Land Surface— PBL Dynamics

With a combined approach using the modified two-layer bucket model of soil moisture dynamics and the empirical relationships developed in this study, we estimate the PBL_h for six possible scenarios. The total precipitation modeled for the current regime scenario S1 (352 mm; Table 5 and Figure 8) was consistent with observed data from our study site ($\sim 350 \text{ mm}$). Total S5 precipitation was higher compared to the other scenarios (360 mm; Table 5), while the PBL_h was the lowest ($PBL_h(\theta_{sh}, \alpha)$, 2,542 m; Table 5).

Consistent with previous research (Kurz & Small, 2007), for all precipitation scenarios, shallow soil moisture mimics the pulse dynamics of precipitation (e.g., Figures 8–10); shallow moisture ranged from 6.2% to

Table 5
Total Precipitation (PPT), Shallow Soil Moisture (θ_{sh}), Deep Soil Moisture (θ_d), Albedo (α), Planetary Boundary Layer Height (PBL_h) Based on the Three Empirical Relationships for Each of the Six Precipitation Scenarios: S1, Current Regime; S2, 20% Decrease in Overall Precipitation; S3, 20% Decrease in Overall Precipitation and a 30% Decrease in Frequency; S4, 20% Decrease in Overall Precipitation and a 30% Increase in Frequency; S5, 12% Decrease in Winter Precipitation; and S6, 20% Increase in Winter Precipitation and a 20% Decrease in Summer Precipitation

	PPT (mm)	θ_{sh} ($\text{m}^3 \text{ m}^{-3}$)	θ_d ($\text{m}^3 \text{ m}^{-3}$)	α (%)	PBL_h (θ_{sh}, α)	PBL_h (θ_{sh}, θ_d)	PBL_h ($\theta_{sh}, \theta_d, \alpha$)
S1	352	0.079 ± 0.03	0.096 ± 0.006	19.11 ± 0.98	$2,557 \pm 450$	$2,337 \pm 586$	$2,627 \pm 641$
S2	239	0.069 ± 0.02	0.094 ± 0.005	19.44 ± 0.58	$2,695 \pm 353$	$2,487 \pm 489$	$2,780 \pm 548$
S3	290	0.074 ± 0.02	0.095 ± 0.006	19.26 ± 0.66	$2,590 \pm 375$	$2,384 \pm 516$	$2,676 \pm 575$
S4	275	0.072 ± 0.02	0.095 ± 0.005	19.33 ± 0.53	$2,615 \pm 338$	$2,409 \pm 481$	$2,704 \pm 542$
S5	360	0.081 ± 0.03	0.096 ± 0.007	19.06 ± 1.06	$2,542 \pm 471$	$2,320 \pm 596$	$2,609 \pm 656$
S6	307	0.075 ± 0.02	0.095 ± 0.006	19.23 ± 0.62	$2,566 \pm 378$	$2,359 \pm 510$	$2,650 \pm 568$

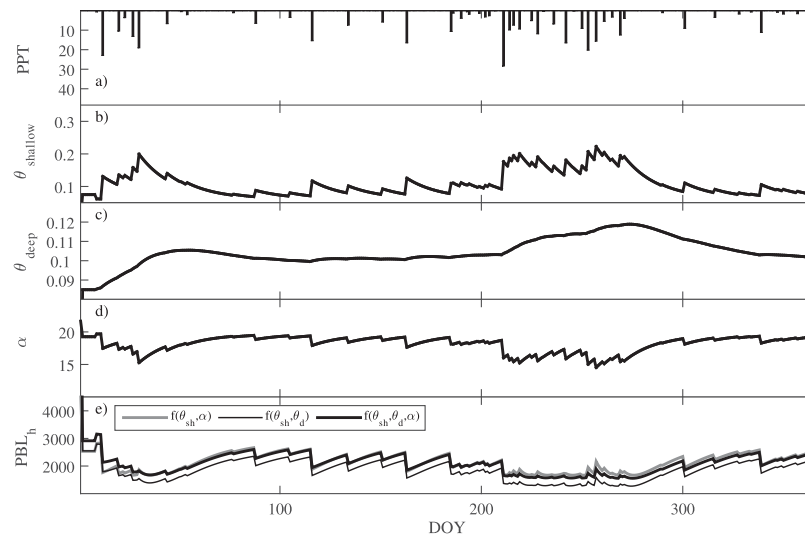


Figure 8. Land surface and PBL_h dynamics based on modeling approach using historical data from DAYMET (S1); PPT is precipitation in mm, θ_{sh} is shallow soil moisture, and θ_d is deep soil moisture in $m^3 m^{-3}$, α is albedo in %, and PBL_h is planetary boundary layer height in m.

22.3% and deep soil moisture ranged from 8.5% to 11.9% increasing after large storms and collections of smaller storms. Overall, a 20% decrease in total annual precipitation (S2, S3, and S4) resulted in less average shallow and deep soil moisture, regardless of the frequency of precipitation (Table 5); however, a decrease in winter precipitation (S5) resulted in slightly more annual precipitation (360 mm) which resulted in 2% more shallow moisture and a 12 m lower PBL , while an increase of winter and decrease of summer rainfall (S6) resulted in a decrease in annual precipitation. In water-limited regions, soil moisture responses follow precipitation regimes (e.g., Calvet & Noilhan, 2000; Kurc & Small, 2007; Pumo et al., 2008), therefore we argue that the response for each scenario is in reasonable ranges, and that the dynamics, especially for shallow moisture, have been well represented.

In S1, the current precipitation regime, albedo ranged from 14.6% to 19.7% (Figure 8); however, the largest range (12.51%–19.62%) was for S6 (Figure 10). This is reasonable given that the changes made to the precipitation regime essentially seasonally maximize wet and dry conditions. Average albedo was the lowest

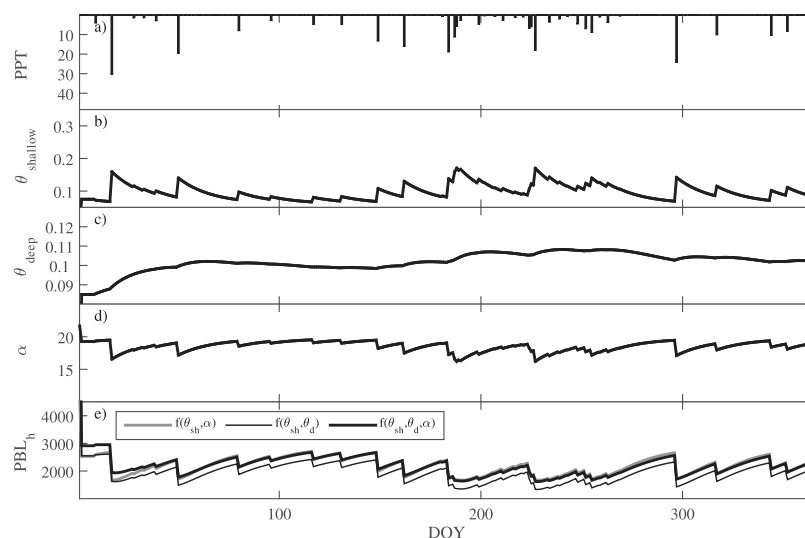


Figure 9. Land surface and PBL_h dynamics under scenario S3 (a decrease in precipitation and an increase in frequency); PPT is precipitation in mm, θ_{sh} is shallow soil moisture and θ_d is deep soil moisture in $m^3 m^{-3}$, α is albedo in %, and PBL_h is planetary boundary layer height in m.

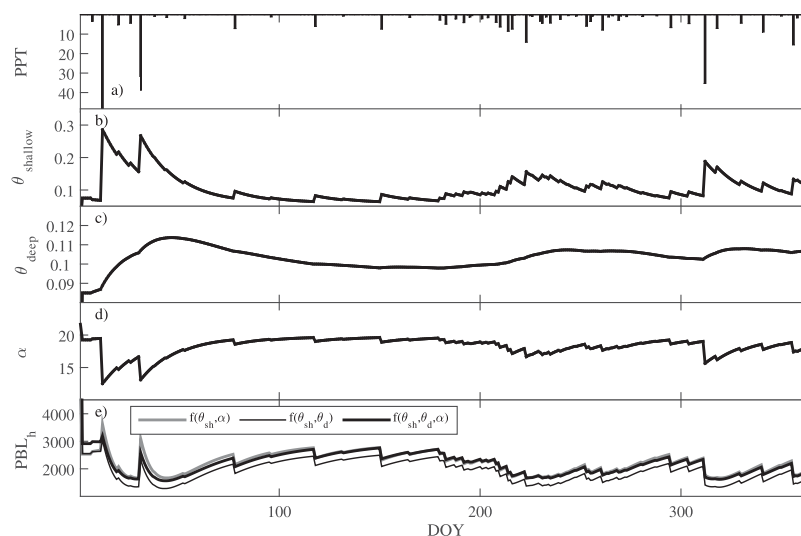


Figure 10. Land surface and PBL_h dynamics under scenario S6 (an increase in winter precipitation and a decrease in the summer precipitation); PPT is precipitation in mm, θ_{sh} is shallow soil moisture and θ_d is deep soil moisture in $m^3 m^{-3}$, α is albedo in %, and PBL_h is planetary boundary layer height in m.

for the scenario with less winter precipitation S5 (19.05%; Table 5) and the highest for an overall decrease in precipitation S2 and S4 (19.44% and 19.33%; Table 5). This is reasonable as we expect albedo to increase with drier soils (Sanchez-Mejia & Papuga, 2014; Small & Kurc, 2003). Notably, average albedo values between the scenarios are not very different (Table 5, range difference = 0.38%), and previous studies for this study area show similar annual values, annual albedo can show low interannual variability unless there is an extreme anomaly (Boussetta et al., 2015). However, it is the temporal dynamics of the interactions between albedo and soil moisture and also vegetation cover (Sanchez-Mejia et al., 2014) that will be important to consider when exploring land surface–atmosphere interactions under any future precipitation scenarios including extreme events.

The average PBL_h varied depending on the empirical relationship used (Table 1), developing the least when it was a function of shallow and deep soil moisture (2,320 m; Table 5) and the most when it was a function of soil moisture shallow, deep, and albedo (2,780 m; Table 5). Average PBL_h was highest under S2 with a 20% decrease in overall precipitation when estimated as a function of shallow and deep soil moisture and albedo (Table 5) and was the lowest in the scenario representing less winter precipitation but a normal monsoon S5 (2,542 m; Table 5). This is consistent with previous studies which have suggested that drier conditions influence soil moisture in such a way that results in a higher PBL_h (Idso, 1972; Pitman, 2003; Sanchez-Mejia & Papuga, 2014). In general, the PBL_h tends to rise throughout the spring with a decrease at the onset of the wet season before it begins to rise again around day 300 (Figures 8–10); this is especially apparent in scenario S1, the current precipitation regime (Figure 8). Decreases in summer precipitation (e.g., S3, Figure 9; and S6, Figure 10) tend to inhibit the post wet season recovery of the PBL_h as compared to the current precipitation regime, suggesting that decreased summer precipitation is likely to create a positive feedback that would further reduce precipitation (Charney, 1975; Douville et al., 2001; Rowell et al., 1995). PBL_h ranges are largest in scenario S6 (increase in winter precipitation and decrease in summer precipitation) largely due to dips and then large increases in PBL_h observed in the winter that are responses to two large winter storms that wet the shallow and deep layer much more than the winter storms in the other precipitation scenarios. This suggests that future increases in winter precipitation may create a more dynamic PBL_h , with the possibility of creating conditions conducive to a positive feedback that could promote increased precipitation in that winter season that might not be possible in other seasons because of the nature of the winter storms and how they wet the soil (e.g., Findell & Eltahir, 1997; Zhu et al., 2009).

To develop further insights on the influence of shallow and deep moisture on linkages between the land surface and the atmosphere, we classified each day of each scenario into one of four soil moisture Cases (see section 2.1). Overall, Case 1 (dry shallow and dry deep soil layers) is the most common classification

Table 6
Case Analysis Showing Number of Days, Mean Albedo, and Mean Planetary Boundary Layer Height, for Each Scenario and Case Based on the Two-Layer Soil Moisture Approach

		Case 1	Case 2	Case 3	Case 4
S1	Days	283	49	27	6
	Albedo (%)	19.5	17.7	17.4	18.8
	PBL_h (m)	2,747	1,874	1,799	2,285
S2	Days	308	36	14	7
	Albedo (%)	19.6	18	17.2	18.1
	PBL_h (m)	2,845	1,914	1,793	2,263
S3	Days	300	32	28	5
	Albedo (%)	19.7	17.7	17.6	18.8
	PBL_h (m)	2,859	1,849	1,822	2,270
S4	Days	322	43	–	–
	Albedo (%)	19.5	18.0	–	–
	PBL_h (m)	2,709	1,938	–	–
S5	Days	259	38	56	12
	Albedo (%)	19.5	17.7	17.4	18.8
	PBL_h (m)	2,730	1,948	1,828	2,269
S6	Days	297	32	34	2
	Albedo (%)	19.5	17.6	17.8	18.6
	PBL_h (m)	2,718	1,867	1,878	2,159

condition. As expected, the occurrence of the Case 1 condition becomes more frequent for scenarios with a decrease in 20% total rainfall than for the current precipitation regime (S1), regardless of whether it is only decrease in rainfall (S2) or it is a decrease associated with less frequent larger events (S3) or more frequent smaller storms (S4) (Table 6; ~50%, ~40%, and ~50%, respectively). Further, the occurrence of Case 1 conditions is more common with an overall decrease in precipitation and increase in frequency (S4; Table 6; ~50%). Occurrences of Case 4 conditions (dry shallow and wet deep soil layers) become less common in all scenarios where overall precipitation decreases (S2, S3, S4, and S5; Table 6) (Table 6). Unlike for the other scenarios, for scenario S6 (increase in winter precipitation but decrease in summer precipitation), the number of occurrences of Case 4 does not change relative to S1, the current precipitation regime (Table 6). Despite shifts in Cases within the scenarios, Case 2 (wet shallow and dry deep soil layers) is the most common condition after Case 1 except in S5 and S6 in which Case 3 is the second most common, and in some scenarios Case 3 and 4 are not present (Table 6). The Cases reflect the dynamic nature of soil moisture and are linked to land surface processes such as vegetation greenness, which has been established as an important link when analyzing soil moisture and albedo (Choudhury & Ghosh, 2014), and its ultimately influence on the PBL_h (Sanchez-Mejia & Papuga, 2014; Sanchez-Mejia et al., 2014).

While it is beyond the scope of this study, one value in our approach is that it opens the door for testing hypotheses about possible mechanisms that relate the precipitation scenarios to the changes in the soil moisture cases. For instance, what mechanisms can result in an overall decrease in precipitation (e.g., S2) having no change in Case 4 conditions (dry shallow layer, wet deep layer). One could hypothesize, for instance, that this is because despite having less overall rainfall, the ratio of large to small storms could be greater. Clearly, the Cases are intertwined, e.g., Case 4 conditions only happen after Case 3 conditions and are influenced by season. Therefore, hypotheses about the mechanisms within the scenarios and their effect on Case classification would really need to be strongly developed.

Overall, ecosystem albedo is generally low when soil moisture is present in the shallow layer (Cases 2 and 3) for all scenarios (Table 6). Albedo is lowest overall in Case 2 for scenario S6 (17.6%; Table 6) and highest overall in Case 1 for the scenario S3 (Table 6; 19.7%). The PBL_h generally develops more for the driest conditions (Case 1) and least during the wettest conditions (Case 3) for all scenarios. This is reasonable as the PBL_h will develop in direct response to the amount of moisture at the surface (Domingo et al., 1999; Santanello et al., 2007). On average, the PBL_h was highest in Case 1 under scenario S3 (Table 6; 2,859 m) and lowest in Case 3 under scenario S2 (Table 6; 1,793 m). These results suggest in addition to changes in the total amount of rainfall that the timing and frequency of precipitation events will play a critical role in the development of the planetary boundary layer and thus future land surface-atmosphere interactions.

4. Summary

Here we explore the application of a two-layer conceptual soil moisture framework to develop empirical relationships between soil moisture, albedo, and the planetary boundary layer height (Santanello et al., 2005) using a modified bucket model approach. Further, we use this approach to explore the impacts of potential changes in precipitation regime on the land surface-atmospheric interactions. This is important because processes in the surface such as vegetation green-up have an influence on roughness, and transpiration which ultimately impact the *PBL* development.

Our results show that a two-layer approach is feasible and that using this approach, we can simulate both shallow and deep layer soil moisture dynamics for use in multiple applications. Notably, however, shallow soil moisture is better represented than deep soil moisture (Figure 5), leaving room for further improvement, perhaps through the inclusion of hydraulic redistribution (Guswa, 2012; Nadezhkina et al., 2010; Ryel et al., 2004). We argue that there is great value in developing empirical relationships to simulate atmospheric processes in the *PBL*, because variables such as soil moisture and albedo are more readily available in space and time via ground measurements and/or remote sensing than more traditional atmospheric variables such as atmospheric stability; our results support the approach of using soil moisture and albedo for estimating PBL_h (e.g., equations (8)–(10) and Figure 7). The simplicity of this approach also enables the exploration of potential precipitation regime changes based on relevant literature. Our results highlight while changes in total or average annual precipitation may have important climate implications, changes in frequency and intensity of precipitation are also important to consider for the development of the PBL_h and its implications for land surface-atmosphere feedbacks.

Importantly, understanding of the *PBL* dynamics are important for planning and natural resource management applications because of their relationship to processes such as particle (i.e., soils, pollutants) dispersion (Zilitinkevich & Baklanov, 2002) and dynamics in urban systems (Luley et al., 2002).

Acknowledgments

This research was supported in part by University of Arizona College of Agriculture and Life Sciences (CALs), The Arizona University System Technology and Research Initiative Fund (TRIF), The University of Arizona Office of the Vice President for Research (VPR), SAHRA (Sustainability of Semi-Arid Hydrology and Riparian area) under the STC Program of the National Science Foundation (NSF), NSF CAREER Award # EAR-1255013, the UA Springfield Scholarship for Graduate Research in Rangelands, the UA William A. Calder III PhD Scholarship for Mexican graduate students focused in conservation, and the UA Kel M. Fox Watershed Scholarship. Data used in this study are available at the Ameriflux website: <https://ameriflux.lbl.gov/or> by contacting the authors. The authors thank J. Santanello and X. Zeng for their suggestions in the approach of the analysis. The manuscript has also benefited greatly from the input of three anonymous reviewers.

References

- Arya, P. S. (2001). *Introduction to micrometeorology*. Cambridge, MA: Academic Press.
- Asbjornsen, H., Goldsmith, G. R., Alvarado-Barrientos, M. S., Rebel, K., Van Osch, F. P., Rietkerk, M., . . . Dawson, T. E. (2011). Ecohydrological advances and applications in plant-water relations research: A review. *Journal of Plant Ecology*, 4(1–2), 3–22.
- Baldocchi, D., Falge, E., Gu, L., Olson, R., Hollinger, D., Running, S., . . . Wofsy, S. (2001). FLUXNET: A new tool to study the temporal and spatial variability of ecosystem-scale carbon dioxide, water vapor, and energy flux densities. *Bulletin of the American Meteorological Society*, 82(11), 2415–2434.
- Basara, J., & Crawford, K. (2002). Linear relationships between root-zone soil moisture and atmospheric processes in the planetary boundary layer. *Journal of Geophysical Research*, 107(D15). <https://doi.org/10.1029/2001JD000633>
- Betts, A. K., & Ball, J. H. (1994). Budget analysis of FIFE-1987 sonde data. *Journal of Geophysical Research*, 99(D2), 3655–3666.
- Blanken, P. D., Black, T. A., Neumann, H. H., Hartog, G. D., Yang, P. C., Nesic, Z., . . . Novak, M. D. (1998). Turbulent flux measurements above and below the overstory of a boreal aspen forest. *Boundary-Layer Meteorology*, 89(1), 109–140.
- Bonser, J. D., Unny, T. E., & Singhal, K. (1985). A marked Poisson-process model of summer rainfall in southern Ontario. *Canadian Journal of Civil Engineering*, 12(4), 886–898.
- Boulet, G., Braud, I., & Vauclin, M. (1997). Study of the mechanisms of evaporation under arid conditions using a detailed model of the soil-atmosphere continuum. Application to the EFEDA I experiment. *Journal of Hydrology*, 193(1–4), 114–141.
- Boussetta, S., Balsamo, G., Dutra, E., Beljaars, A., & Albergel, C. (2015). Assimilation of surface albedo and vegetation states from satellite observations and their impact on numerical weather prediction. *Remote Sensing of Environment*, 163, 111–126.
- Breshears, D., Myers, O., Johnson, S., Meyer, C., & Martens, S. (1997). Differential use of spatially heterogeneous soil moisture by two semi-arid woody species: *Pinus edulis* and *Juniperus monosperma*. *Journal of Ecology*, 85(3), 289–299.
- Caldwell, M. M., Dawson, T. E., & Richards, J. H. (1998). Hydraulic lift: Consequences of water efflux from the roots of plants. *Oecologia*, 113(2), 151–161.
- Calvet, J. C., & Noilhan, J. (2000). From near-surface to root-zone soil moisture using year-round data. *Journal of Hydrometeorology*, 1(5), 393–411.
- Cavanaugh, M. L., Kurc, S. A., & Scott, R. L. (2011). Evapotranspiration partitioning in semiarid shrubland ecosystems: A two-site evaluation of soil moisture control on transpiration. *Ecohydrology*, 4(5), 671–681.
- Caylor, K. K., Manfreda, S., & Rodriguez-Iturbe, I. (2005). On the coupled geomorphological and ecohydrological organization of river basins. *Advances in Water Resources*, 28(1), 69–86.
- Chahine, M. T. (1992). The hydrological cycle and its influence on climate. *Nature*, 359(6394), 373–380.
- Charney, J. (1975). Dynamics of deserts and drought in the Sahel. *Quarterly Journal of the Royal Meteorological Society*, 101(428), 193–202.
- Chen, F., & Dudhia, J. (2001). Coupling an advanced land surface-hydrology model with the Penn State-NCAR MM5 modeling system. Part I: Model implementation and sensitivity. *Monthly Weather Review*, 129(4), 569–585.
- Choudhury, I., & Ghosh, R. (2014). Spatio-temporal coupling of land-surface and energy balance parameters with monsoon rainfall using remote-sensing technology. *International Journal of Remote Sensing*, 35(2), 532–553.
- Clapp, R., & Hornberger, G. (1978). Empirical equations for some soil hydraulic properties. *Water Resources Research*, 14(4), 601–604.
- Claussen, M. (1997). Modeling bio-geophysical feedback in the African and Indian monsoon region. *Climate Dynamics*, 13(4), 247–257.

- Coen, M. C., Praz, C., Haefele, A., Ruffieux, D., Kaufmann, P., & Calpini, B. (2014). Determination and climatology of the planetary boundary layer height above the Swiss plateau by in situ and remote sensing measurements as well as by the COSMO-2 model. *Atmospheric Chemistry and Physics*, *14*(23), 13205–13221.
- Cosby, B. J., Hornberger, G. M., Clapp, R. B., & Ginn, T. R. (1984). A statistical exploration of the relationships of soil moisture characteristics to the physical properties of soils. *Water Resources Research*, *20*(6), 682–690.
- Davis, K. J., Gamage, N., Hagelberg, C. R., Kiemle, C., Lenschow, D. H., & Sullivan, P. P. (2000). An objective method for deriving atmospheric structure from airborne lidar observations. *Journal of Atmospheric and Oceanic Technology*, *17*(11), 1455–1468.
- Dekker, S., Rietkerk, M., & Bierkens, M. (2007). Coupling microscale vegetation-soil water and macroscale vegetation-precipitation feedbacks in semiarid ecosystems. *Global Change Biology*, *13*(3), 671–678.
- Domingo, F., Villagarcía, L., Brenner, A. J., & Puigdefabregas, J. (1999). Evapotranspiration model for semi-arid shrub-lands tested against data from SE Spain. *Agricultural and Forest Meteorology*, *95*(2), 67–84.
- Douville, H., Chauvin, F., & Broqua, H. (2001). Influence of soil moisture on the Asian and African monsoons. Part I: Mean monsoon and daily precipitation. *Journal of Climate*, *14*(11), 2381–2403.
- Findell, K. L., & Eltahir, E. A. B. (1997). An analysis of the soil moisture-rainfall feedback, based on direct observations from Illinois. *Water Resources Research*, *33*(4), 725–735.
- Garfin, G., Franco, G., Blanco, G., Comrie, A., Gonzalez, P., Piechota, T., . . . Waskom, R. (2014). Chapter 20: Southwest. In J. Melillo, T. Richmond, & G. Yohe (Eds.), *Climate change impacts in the United States: The third national climate assessment* (pp. 462–486). Washington, DC: Global Change Research Program.
- Ghan, S. J., Liljegren, J. C., Shaw, W. J., Hubbe, J. H., & Doran, J. C. (1997). Influence of subgrid variability on surface hydrology. *Journal of Climate*, *10*(12), 3157–3166.
- Giorgi, F., & Avissar, R. (1997). Representation of heterogeneity effects in earth system modeling: Experience from land surface modeling. *Reviews of Geophysics*, *35*(4), 413–437.
- Griffin, D., Woodhouse, C. A., Meko, D. M., Stahle, D. W., Faulstich, H. L., Carrillo, C., . . . Leavitt, S. W. (2013). North American monsoon precipitation reconstructed from tree-ring latewood. *Geophysical Research Letters*, *40*, 954–958. <https://doi.org/10.1002/grl.50184>
- Guswa, A. J. (2012). Canopy vs. roots: Production and destruction of variability in soil moisture and hydrologic fluxes. *Vadose Zone Journal*, *11*(3), 13.
- Guswa, A. J., Celia, M. A., & Rodriguez-Iturbe, I. (2002). Models of soil moisture dynamics in ecohydrology: A comparative study. *Water Resources Research*, *38*(9), 1166. <https://doi.org/10.1029/2001WR000826>
- Gutzler, D. S. (2000). Covariability of spring snowpack and summer rainfall across the southwest United States. *Journal of Climate*, *13*(22), 4018–4027.
- Henderson-Sellers, A. (1993). Continental vegetation as a dynamic component of a global climate model—A preliminary assessment. *Climatic Change*, *23*(4), 337–377.
- Hernandez, C., Drobinski, P., & Turquety, S. (2015). Impact of wildfire-induced land cover modification on local meteorology: A sensitivity study of the 2003 wildfires in Portugal. *Atmospheric Research*, *164*, 49–64.
- Idso, S. (1972). A note on some recently proposed mechanisms of genesis of deserts. *Quarterly Journal of the Royal Meteorological Society*, *103*(436), 369–370.
- Jackson, R., Idso, S., & Reginato, R. (1976). Calculation of evaporation rates during the transition from energy-limiting to soil-limiting phases using albedo data. *Water Resources Research*, *12*(1), 23–26.
- Katul, G., Porporato, A., & Oren, R. (2007). Stochastic dynamics of plant-water interactions. *Annual Review of Ecology, Evolution, and Systematics*, *38*, 767–791.
- Kunkel, K., Stevens, L., Stevens, S., Sun, L., Janssen, E., Wuebbles, D., . . . Dobson, J. (2013). *Regional climate trends and scenarios for the US national climate assessment. Part 5. Climate of the southwest U.S.* (NOAA Technical Report NESDIS 142-5). Washington, DC: U.S. Department of Commerce, National Ocean and Atmospheric Administration.
- Kurc, S., & Benton, L. (2010). Digital image-derived greenness links deep soil moisture to carbon uptake in a creosotebush-dominated shrubland. *Journal of Arid Environments*, *74*(5), 585–594.
- Kurc, S., & Small, E. (2007). Soil moisture variations and ecosystem-scale fluxes of water and carbon in semiarid grassland and shrubland. *Water Resources Research*, *43*, W06416. <https://doi.org/10.1029/2006WR005011>
- Laio, F., Porporato, A., Ridolfi, L., & Rodriguez-Iturbe, I. (2001). Plants in water-controlled ecosystems: Active role in hydrologic processes and response to water stress—II. *Probabilistic soil moisture dynamics. Advances in Water Resources*, *24*(7), 707–723.
- LeMone, M., Chen, F., Alfieri, J., Cuenca, R., Hagimoto, Y., Blanken, P., . . . Grossman, R. (2007). NCAR/CU surface, soil, and vegetation observations during the international H₂O project 2002 field campaign. *Bulletin of the American Meteorological Society*, *88*(1), 65–81.
- Liu, B., Phillips, F., Hoines, S., Campbell, A., & Sharma, P. (1995). Water-movement in desert soil traced by hydrogen and oxygen isotopes, chloride, and CL-36, Southern Arizona. *Journal of Hydrology*, *168*(1–4), 91–110.
- Luley, C. J., Bond, J., & Agencies, C. (2002). *A plan to integrate management of urban trees into air quality planning*. Naples, NY: Davey Resource Group.
- Lyon, S. W., Dominguez, F., Gochis, D. J., Kucera, P. A., Salzmann, N., Schmidli, J., . . . Salvucci, G. D. (2008). Coupling terrestrial and atmospheric water dynamics to improve prediction in a changing environment. *Bulletin of the American Meteorological Society*, *89*(9), 1275–1279.
- Manabe, S. (1969). Climate and the ocean circulation I. The atmospheric circulation and the hydrology of the earth's surface. *Monthly Weather Review*, *97*, 739–774.
- Miller, R., Slingo, A., Barnard, J., & Kassianov, E. (2009). Seasonal contrast in the surface energy balance of the Sahel. *Journal of Geophysical Research*, *114*, D00E05. <https://doi.org/10.1029/2008JD010521>
- Mills, R. (1990). Remote sensing science for the nineties. In *IGARSS '90. 10th Annual International Geoscience and Remote Sensing Symposium* (Vol. I, pp. 2488). New York, NY: IEEE.
- Moncrieff, J., Jarvis, P., & Valentini, R. (2000). Canopy fluxes. In O. Sala, R. Jackson, H. Mooney, & R. Howarth (Eds.), *Methods in ecosystem science* (pp. 161–180). New York, NY: Springer-Verlag.
- Moran, M., Scott, R., Keefer, T., Emmerich, W., Hernandez, M., Nearing, G., . . . O'Neill, P. (2009). Partitioning evapotranspiration in semiarid grassland and shrubland ecosystems using time series of soil surface temperature. *Agricultural and Forest Meteorology*, *149*(1), 59–72.
- Mueller, B., Seneviratne, S. I., Jimenez, C., Corti, T., Hirschi, M., Bals, G., . . . Zhang, Y. (2011). Evaluation of global observations-based evapotranspiration datasets and IPCC AR4 simulations. *Geophysical Research Letters*, *38*, L06402. <https://doi.org/10.1029/2010GL046230>
- Nadezhkina, N., David, T. S., David, J. S., Ferreira, M. I., Dohnal, M., Tesar, M., . . . Morales, D. (2010). Trees never rest: The multiple facets of hydraulic redistribution. *Ecohydrology*, *3*(4), 431–444.

- NAST & USGCRP. (2000). *Climate change impacts on the United States: The potential consequences of variability and change*. New York, NY: Cambridge University Press.
- Nemani, R., Pierce, L., Running, S., & Goward, S. (1993). Developing satellite-derived estimate of surface moisture status. *Journal of Applied Meteorology and Climatology*, 32(3), 548–557.
- Otterman, J., Novak, M. D., & Starr, D. O. (1993). Turbulent heat-transfer from a sparsely vegetated surface—2-component representation. *Boundary-Layer Meteorology*, 64(4), 409–420.
- Pal, J. S., & Eltahir, E. A. (2001). Pathways relating soil moisture conditions to future summer rainfall within a model of the land–atmosphere system. *Journal of Climate*, 14(6), 1227–1242.
- Pitman, A. (2003). The evolution of, and revolution in, land surface schemes designed for climate models. *International Journal of Climatology*, 23(5), 479–510.
- Pleim, J. E. (2007). A combined local and nonlocal closure model for the atmospheric boundary layer. Part I: Model description and testing. *Journal of Applied Meteorology and Climatology*, 46(9), 1383–1395.
- Porporato, A., Daly, E., & Rodriguez-Iturbe, I. (2004). Soil water balance and ecosystem response to climate change. *American Naturalist*, 164(5), 625–632.
- Porporato, A., D'odorico, P., Laio, F., Ridolfi, L., & Rodriguez-Iturbe, I. (2002). Ecohydrology of water-controlled ecosystems. *Advances in Water Resources*, 25(8–12), 1335–1348.
- Pumo, D., Viola, F., & Noto, L. V. (2008). Ecohydrology in Mediterranean areas: A numerical model to describe growing seasons out of phase with precipitations. *Hydrology and Earth System Sciences*, 12(1), 303–316.
- Quintanar, A. I., Mahmood, R., Loughrin, J., & Lovanh, N. C. (2008). A coupled MMS-NOAH land surface model-based assessment of sensitivity of planetary boundary layer variables to anomalous soil moisture conditions. *Physical Geography*, 29(1), 54–78.
- Randall, D. A., Wood, R. A., Bony, S., Colman, R., Fichefet, T., Fyfe, J., . . . Srinivasan, J. (2007). Climate models and their evaluation. In *Climate change 2007: The physical science basis. Contribution of working group I to the fourth assessment report of the IPCC (FAR)* (pp. 589–662). Cambridge, UK: Cambridge University Press.
- Raz-Yaseef, N., Yakir, D., Schiller, G., & Cohen, S. (2012). Dynamics of evapotranspiration partitioning in a semi-arid forest as affected by temporal rainfall patterns. *Agricultural and Forest Meteorology*, 157, 77–85.
- Reynolds, J. F., Kemp, P. R., & Tenhunen, J. D. (2000). Effects of long-term rainfall variability on evapotranspiration and soil water distribution in the Chihuahuan Desert: A modeling analysis. *Plant Ecology*, 150(1–2), 145–159.
- Rietkerk, M., Boerlijst, M. C., van Langevelde, F., HilleRisLambers, R., van de Koppel, J., Kumar, L., . . . de Roos, A. M. (2002). Self-organization of vegetation in arid ecosystems. *American Naturalist*, 160(4), 524–530.
- Rihani, J. F., Chow, F. K., & Maxwell, R. M. (2015). Isolating effects of terrain and soil moisture heterogeneity on the atmospheric boundary layer: Idealized simulations to diagnose land-atmosphere feedbacks. *Journal of Advances in Modeling Earth Systems*, 7(2), 915–937.
- Rodriguez-Iturbe, I. (2000). Ecohydrology: A hydrologic perspective of climate-soil-vegetation dynamics. *Water Resources Research*, 36(1), 3–9.
- Rodriguez-Iturbe, I., D'odorico, P., Porporato, A., & Ridolfi, L. (1999a). On the spatial and temporal links between vegetation, climate, and soil moisture. *Water Resources Research*, 35(12), 3709–3722.
- Rodriguez-Iturbe, I., Porporato, A., Ridolfi, L., Isham, V., & Cox, D. (1999b). Probabilistic modelling of water balance at a point: The role of climate, soil and vegetation. *Proceedings of the Royal Society A: Mathematical Physical and Engineering Sciences*, 455(1990), 3789–3805.
- Rowell, D. P., Folland, C. K., Maskell, K., & Ward, M. N. (1995). Variability of summer rainfall over tropical North-Africa (1906–92)—Observations and modeling. *Quarterly Journal of the Royal Meteorological Society*, 121(523), 669–704.
- Ryel, R. J., Leffler, A. J., Peek, M. S., Ivans, C. Y., & Caldwell, M. M. (2004). Water conservation in *Artemisia tridentata* through redistribution of precipitation. *Oecologia*, 141(2), 335–345.
- Sala, O. E., & Lauenroth, W. K. (1982). Small rainfall events: An ecological role in semiarid regions. *Oecologia*, 53(3), 301–304.
- Salvucci, G. D. (2001). Estimating the moisture dependence of root zone water loss using conditionally averaged precipitation. *Water Resources Research*, 37(5), 1357–1365.
- Sanchez-Mejia, Z. M., & Papuga, S. A. (2014). Observations of a two-layer soil moisture influence on surface energy dynamics and planetary boundary layer characteristics in a semiarid shrubland. *Water Resources Research*, 50, 306–317. <https://doi.org/10.1002/2013WR014135>
- Sanchez-Mejia, Z. M., Papuga, S. A., Swetish, J. B., van Leeuwen, W. J. D., Szutu, D., & Hartfield, K. (2014). Quantifying the influence of deep soil moisture on ecosystem albedo: The role of vegetation. *Water Resources Research*, 50, 4038–4053. <https://doi.org/10.1002/2013WR014150>
- Sandeep, A., Rao, T. N., Ramkiran, C. N., & Rao, S. V. B. (2014). Differences in atmospheric boundary-layer characteristics between wet and dry episodes of the Indian summer monsoon. *Boundary-Layer Meteorology*, 153(2), 217–236.
- Santanello, J., Friedl, M., & Ek, M. (2007). Convective planetary boundary layer interactions with the land surface at diurnal time scales: Diagnostics and feedbacks. *Journal of Hydrometeorology*, 8(5), 1082–1097.
- Santanello, J., Friedl, M., & Kustas, W. (2005). An empirical investigation of convective planetary boundary layer evolution and its relationship with the land surface. *Journal of Applied Meteorology*, 44(6), 917–932.
- Scheffer, M., Holmgren, M., Brovkin, V., & Claussen, M. (2005). Synergy between small- and large-scale feedbacks of vegetation on the water cycle. *Global Change Biology*, 11(7), 1003–1012.
- Scott, R., Cable, W., & Hultine, K. (2008). The ecohydrologic significance of hydraulic redistribution in a semiarid savanna. *Water Resources Research*, 44, W02440. <https://doi.org/10.1029/2007WR006149>
- Scott, R., Huxman, T., Cable, W., & Emmerich, W. (2006). Partitioning of evapotranspiration and its relation to carbon dioxide exchange in a Chihuahuan Desert shrubland. *Hydrological Processes*, 20(15), 3227–3243.
- Seidel, D. J., Ao, C. O., & Li, K. (2010). Estimating climatological planetary boundary layer heights from radiosonde observations: Comparison of methods and uncertainty analysis. *Journal of Geophysical Research*, 115, D16113. <https://doi.org/10.1029/2009JD013680>
- Seneviratne, S., Corti, T., Davin, E., Hirschi, M., Jaeger, E., Lehner, I., . . . Teuling, A. (2010). Investigating soil moisture-climate interactions in a changing climate: A review. *Earth-Science Reviews*, 99(3–4), 125–161.
- Shuttleworth, W. (1993). Evaporation. In D. Maidement (Ed.), *Handbook of hydrology* (pp. 53). New York, NY: McGraw-Hill.
- Shuttleworth, W. (2012). *Terrestrial hydrometeorology* (441 pp.). Oxford, UK: Wiley-Blackwell.
- Small, E. E., & Kurc, S. A. (2003). Tight coupling between soil moisture and the surface radiation budget in semiarid environments: Implications for land-atmosphere interactions. *Water Resources Research*, 39(10), 1278. <https://doi.org/10.1029/2002WR001297>
- Stull, R. (1988). *An introduction to boundary layer meteorology* (pp. 666). Boston, UK: Kluwer Academic Publishers.
- Terink, W., Lutz, A. F., Simons, G. W. H., Immerzeel, W. W., & Droogers, P. (2015). SPHY v2.0: Spatial processes in Hydrology. *Geoscientific Model Development*, 8(7), 2009–2034.

- Thornton, P., Thornton, M., Mayer, B., Wilhelmi, N., Wei, Y., Devarakonda, R., & Cook, R. (2014). *Daymet: Daily surface weather data on a 1-km grid for North America; version 2*. Oak Ridge, TN: Oak Ridge National Laboratory Distributed Active Archive Center. <https://doi.org/10.3334/ORNLDAAC/1219>
- Trenberth, K., Dai, A., Rasmussen, R., & Parsons, D. (2003). The changing character of precipitation. *Bulletin of the American Meteorological Society*, *84*(9), 1205–1217.
- van Keulen, H., & Hillel, D. (1974). Simulation of the study of drying-front phenomenon. *Soil Science*, *118*(4), 270–273.
- Villegas, J., Breshears, D., Zou, C., & Law, D. (2010). Ecohydrological controls of soil evaporation in deciduous drylands: How the hierarchical effects of litter, patch and vegetation mosaic cover interact with phenology and season. *Journal of Arid Environments*, *74*(5), 595–602.
- Wang, L., D'odorico, P., Evans, J. P., Eldridge, D. J., McCabe, M. F., Caylor, K. K., & King, E. G. (2012). Dryland ecohydrology and climate change: Critical issues and technical advances. *Hydrology and Earth System Sciences*, *16*(8), 2585–2603.
- Wei, J., Dirmeyer, P. A., Guo, Z., Zhang, L., & Misra, V. (2010). How much do different land models matter for climate simulation? Part I: Climatology and variability. *Journal of Climate*, *23*(11), 3120–3134.
- Weltzin, J., Loik, M. E., Schwinning, S., Williams, D. G., Fay, P. A., Haddad, B. M., . . . Zak, J. C. (2003). Assessing the response of terrestrial ecosystems to potential changes in precipitation. *Bioscience*, *53*(10), 941–952.
- Western, A. W., Grayson, R. B., Blöschl, G., Willgoose, G. R., & McMahon, T. A. (1999). Observed spatial organization of soil moisture and its relation to terrain indices. *Water Resources Research*, *35*(3), 797–810.
- Yamanaka, T., & Yonetani, T. (1999). Dynamics of the evaporation zone in dry sandy soils. *Journal of Hydrology*, *217*(1–2), 135–148.
- Zeng, N., Neelin, J. D., Lau, K. M., & Tucker, C. J. (1999). Enhancement of interdecadal climate variability in the Sahel by vegetation interaction. *Science*, *286*(5444), 1537–1540.
- Zhao, W., & Li, A. N. (2015). A comparison study on empirical microwave soil moisture downscaling methods based on the integration of microwave-optical/IR data on the Tibetan Plateau. *International Journal of Remote Sensing*, *36*(19–20), 4986–5002.
- Zhu, C. M., Leung, L. R., Gochis, D., Qian, Y., & Lettenmaier, D. P. (2009). Evaluating the influence of antecedent soil moisture on variability of the North American monsoon precipitation in the coupled MMS/VIC modeling system. *Journal of Advances in Modeling Earth Systems*, *1*, 13. <https://doi.org/10.3894/JAMES.2009.1.13>
- Zilitinkevich, S., & Baklanov, A. (2002). Calculation of the height of the stable boundary layer in practical applications. *Boundary-Layer Meteorology*, *105*(3), 389–409.